

Intelligent Environment Design for Indoor Spaces Based on Perception and Behavior Correlation

Xiaomin Xue

School of Design, Fujian University of Technology, Fuzhou 350118, China

E-mail: 13860607040@163.com

Keywords: perception, behavior, PMV indicators, intelligence, fitness

Received: March 19, 2024

With the development of social economy, higher demands have been presented for indoor environment. Intelligent design has become a research hotspot. A Genetic Algorithm-Back Propagation Neural Network model is constructed based on the association between perception and behavior, combined with the Predicted Mean Vote index. Six factors affecting the Predicted Mean Vote indicators are analyzed. However, there are inherent flaws in the Back Propagation Neural Network. Therefore, combined with Genetic Algorithm, a optimized model is built. It had faster convergence speed than the unimproved model. The difference of Predicted Mean Vote was small, with better model fitting effects. The overall model error remained around 0.01, with a maximum error of only 0.022. The model had higher Accuracy, Precision, and F1-score values compared with other models, with values of 97.89%, 96.15%, and 0.896. From the results, it has better generalization ability, which can accurately predict indoor temperature, achieving intelligent control. The model proposed in the study achieves intelligent design of indoor comfort by controlling temperature, providing a reliable foundation for further improving indoor intelligence in subsequent research.

Povzetek: Članek obravnava inteligentno zasnovano notranjih prostorov na osnovi korelacije med zaznavanjem in vedenjem. Avtorica predstavi model genetskega algoritma in povratne nevronske mreže, ki vključuje kazalnik PMV in omogoča hitrejšo konvergenco in natančnejše napovedi.

1 Introduction

With the rapid development of artificial intelligence and Internet of Things technology, intelligent indoor environment design has become a hot research field. The demand for comfortable, energy-saving, and intelligent indoor environments is constantly increasing, which requires advanced technology [1-3]. In the design of indoor intelligent environments, the Predicted Mean Vote (PMV) is a crucial reference standard for evaluating indoor comfort, which comprehensively evaluates factors such as humidity, constant temperature, and air circulation in the indoor environment. However, due to the complexity of indoor environments, a single factor often cannot comprehensively evaluate indoor comfort. Therefore, multiple factors should be comprehensively considered to predict PMV. A Genetic Algorithm-Back Propagation Neural Network (GA-BPNN) prediction method based on perception and behavior correlation is constructed to improve the accuracy and intelligent regulation ability of PMV indicators in indoor intelligent environment design. By analyzing the influencing factors of PMV indicators and combining GA and BPNN, indoor temperature is intelligently predicted. The research has four parts. The first summarizes the research on intelligent design and BPNN, and analyze the research results. The second part is to construct the model and introduce the improved method. The third part is to verify

the performance through comparative experiments. The fourth part is to summarize the experimental results, point out the shortcomings in the research, and propose future research directions. The study will provide a feasible solution for the intelligent design of indoor comfort, providing effective theoretical and methodological support for improving indoor intelligent environment design.

2 Related works

Many scholars have conducted relevant research on intelligent design [4-6]. Wang et al. designed a new car following model for intelligent transportation smoking. Based on the dual speed difference model and the dynamic characteristics of traffic flow, the front distance memory and rear-view effect were analyzed. The linear stability theory was used to describe the evolution characteristic equation of traffic flow density waves. It improved the traffic flow stability and eliminated traffic congestion [7]. Cheng et al. built a behavior prediction model in intelligent butler design. Limited hardware devices were used to collect sufficient information. A Quadro-W learning was developed to predict behavior. This study built a model based on the obtained Quadro-W information. The results indicated that the proposed model could effectively predict the initial environment according to environmental changes, improving the flexibility of the system [8]. Huang et al. proposed a new

intelligent reflection/refraction system. The intelligent surface of high-speed vehicles assisted users in communication, but the rapidly changing channels in communication posed great challenges. The results indicated that the proposed system could effectively work in high mobile communication scenarios and improve the reliability of the output [9]. Zhong et al. proposed the Lego modeling method in the intelligent robot design. Then a Deep Transfer Deterministic Policy Gradient (DT-DPG) was proposed to optimize the efficiency. The results showed that the proposed method could accurately describe indoor layout and channel status. The training efficiency was improved by 30%, which exceeded the DPG [10].

Many scholars have carried out corresponding research on BPNN. Yu et al. designed a calibration method based on BPNN in multi-body dissipative particle dynamics. The study selected three simulation parameters: Attraction and repulsion coefficients A, B, and cutoff radius for repulsion, as well as four static and dynamic properties. The study compared three sampling methods. The proposed method was the most effective in reducing mean square error, which could accurately and effectively determine simulation parameters [11]. Sui et al. proposed a BPNN modeling method in the field of architecture. Virtual reality technology was used to construct models for evaluating building envelope structures and analyzing energy-saving building designs. Building models with different enclosure structures were constructed. In the

identification of heat transfer coefficients in building envelope structures, the error of BPNN was less than 5%. It could effectively save energy, providing a theoretical basis for energy-saving design and evaluation of buildings [12]. Zhang et al. used BPNN to predict fuel ratios in the metallurgical field. The study first analyzed the 55 important production parameters in blast furnace operation. Finally, a comparative experiment was conducted using BPNN and k-nearest neighbor algorithm. From the results, the BPNN could keep the error within 2% and achieve an accuracy of 93.02% [13]. Xu et al. developed a compensation method based on BPNN to solve nonlinear magnetic interference. To obtain sufficient data, a three-dimensional Helmholtz coil was used to recover the magnetic signal. It could lower the Root Mean Square Errors (RMSEs) of the north, east, and vertical components, as well as the total strength to 23.35, 23.58, 27.42, and 29.72nT [14].

Although there have been many achievements in intelligent design and BPNN in previous studies, the BPNN in intelligent design have inherent flaws [15-16]. Therefore, the GA is used to improve BPNN, effectively solving problems such as large errors and susceptibility to local minima. It is expected to update the intelligence of indoor environments, promoting the development and application of intelligent environmental design. The related works table is shown in table 1.

Table 1: The related works table

Study	Method	Technology	Accuracy (%)
Wang et al.	Two-speed difference model	Linear stability theory	94.16
Cheng et al.	Quadro-W Learning	Intelligent butler design	93.33
Huang et al.	Intelligent reflex	Refraction system	95.12
Zhong et al.	Lego modeling	DT-DPG optimization	92.76
Yu et al.	BPNN calibration method	Three types of simulation parameters	94.19
Sui et al.	BPNN modeling method	Virtual reality technology	96.34
Zhang et al.	BPNN prediction method	Blast furnace operating parameters	93.02
Xu et al.	BPNN compensation method	Three-dimensional Helmholtz coil	96.74
Research method	GA-BPNN	Perceived behavioral correlation	97.89

3 Construction of GA-BPNN based on perception and behavior correlation

Based on perceived behavioral correlation, six factors affecting human comfort indicators are analyzed. Then a model is constructed and optimized.

3.1 BPNN based on perception and behavior

Perception is the process in which a person interprets and gradually forms consciousness based on their own experience after perceiving external things. As an internal form of expression, it is caused by the connection between humans and the outside world. Behavior

includes the internal feelings and external language actions that humans possess. The collaborative

mechanism of perception and behavior considers humans as users of the environment. The characteristics and needs of humans directly affect the spatial characteristics exhibited in behavioral activities. There is a mutually penetrating and interconnected relationship among people, behavior, and space. In intelligent environment design, human thermal comfort is a crucial aspect. Thermal comfort refers to the thermal comfort state towards the environment, which is neither cold nor hot. It is applied to describe the satisfaction with indoor thermal environment. The widely used currently is the PMV, which is included in international standards. PMV covers almost all environmental factors that affect comfort. The calculation method for PMV is shown in formula (1).

$$PMV = [0.303e^{-0.036M} + 0.028]L \quad (1)$$

In formula (1), M represents the metabolic rate, (W / m^2). L represents the human heat load. The PMV indicators describe the discrepancy in the real heat dissipation rate and the required heat dissipation to achieve a comfortable state under a given thermal environment. The calculation method for L is shown in formula (2).

$$L = (M - W) - 3.05 \times [5.733 - 0.007(M - W) - P_a] - 0.4(W - M - 58.15) - 0.0173M(5087 - P_a) - 0.0014(34 - t_a) - 3.96 \times 10^{-8} f_{cl}(t_{cl} + 273)^4 - f_{cl}h_c(t_{cl} - t_a) \quad (2)$$

In formula (2), W represents the mechanical work, (W / m^2). P_a represents the partial pressure of air and water vapor, (KPa). t_a represents the air temperature, ($^{\circ}C$). f_{cl} represents the clothing area coefficient. t_{cl} represents the outer surface temperature of clothes, ($^{\circ}C$).

h_c represents the convective heat transfer coefficient, as shown in formula (3).

$$h_c = \begin{cases} 2.38(t_{cl} - t_a)^{0.25} & 2.38(t_{cl} - t_a)^{0.25} > 12.1\sqrt{v_a} \\ 12.1\sqrt{v_a} & 2.38(t_{cl} - t_a)^{0.25} < 12.1\sqrt{v_a} \end{cases} \quad (3)$$

In formula (3), v_a represents the air velocity. If the external work done by a person is zero, PMV can be expressed as formula (4).

$$PMV = f(M, t_a, t_r, I_{cl}, v_a, \varphi) \quad (4)$$

Formula (4) represents the optimal comfortable environment for the human body. If formula (4) is not satisfied, it indicates that the environment is not in the optimal state, but it does not indicate that the environment has reached an uncomfortable level. The indicator that can represent the state of any set of environmental variables using a formula is called the average predictive response PMV. This indicator is divided into seven levels. The meaning of each level is represented in Figure 1.

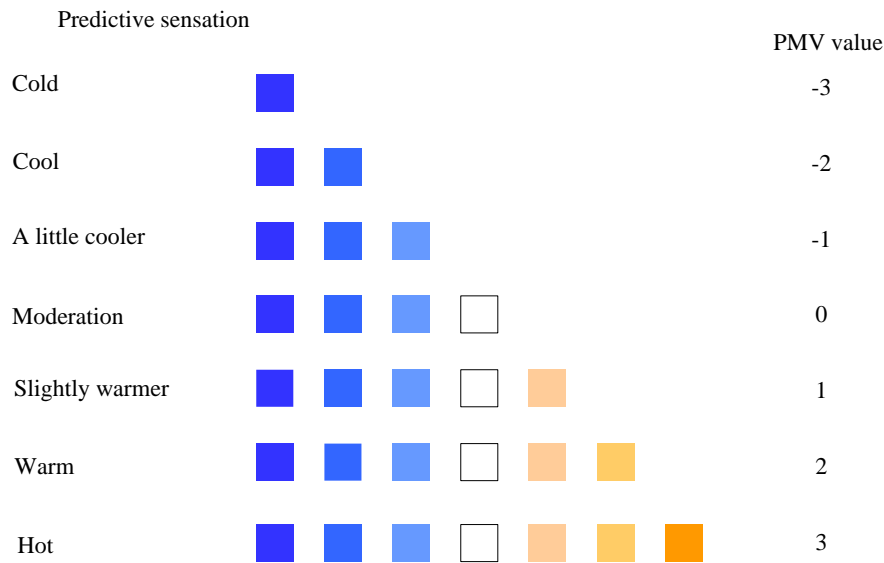


Figure 1: Seven level of PMV thermal comfort

Figure 1 is the seven level indicators of PMV thermal comfort. The PMV equation contains exponential terms, piece-wise functions, parameters, and multiple coupled factors. The calculation process involves multiple

iterations of nonlinear equations. Multiple factors affect human thermal comfort, mainly including physical and human factors, as displayed in Figure 2.

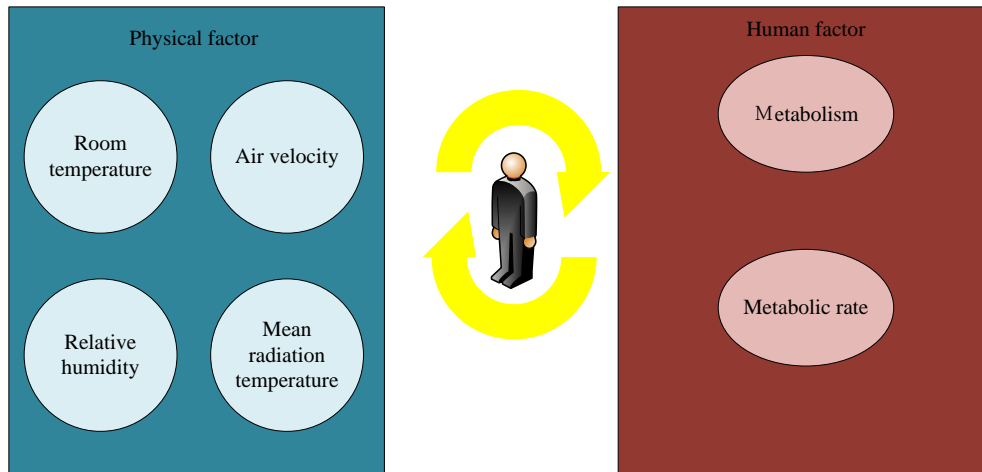


Figure 2: Factors affecting thermal comfort of human body

Figure 2 shows the specific factors. Physical factors refer to the surrounding environment of the human body, including relative humidity, open-air temperature, air flow rate, and mean radiation temperature. Human factors are related to different states of the human body, including metabolic rate, and clothing thermal resistance. The above factors comprehensively affect the human body. When they are in the optimal arrangement and combination, the most comfortable state is achieved. The first problem that must be solved in the intelligent design of indoor temperature is to solve the PMV indicators. Generally speaking, the BPNN is used to calculate index values [17-18]. BPNN is a supervised learning algorithm that simulates the neural network structure of the human brain for pattern recognition and prediction tasks. The model consists of an input layer, a Hidden Layer (HL), and an Output Layer (OL), each of which is composed of multiple neurons. These neurons are connected through weighted connections and undergo nonlinear transformations through activation functions to handle complex nonlinear relationships. The core of BPNN lies in its learning mechanism, which adjusts the weights and thresholds in the network through back propagation algorithms. During the learning, the network first receives input data and calculates the output result through forward propagation. Subsequently, the network calculates the error between the predicted output and the actual target value, and transmits the error signal back to the network through back propagation to adjust weights and thresholds, thereby minimizing the prediction error. The calculation is displayed in formula (5).

$$s_j = \sum_{i=1}^n w_{ij} a_i^k - \theta_j, j = 1, 2, \dots, p \quad (5)$$

In formula (5), w_{ij} represents the connection weights

within $(-1, 1)$. θ_j represents the threshold. a_i^k

represents the input sample. s_j represents the input of each unit. s_j is applied to calculate the output of each unit in the middle layer, as shown in formula (6).

$$b_j = f(s_j), j = 1, 2, \dots, p \quad (6)$$

In formula (6), $f(\cdot)$ represents the transfer function. b_j represents the output of each unit in the middle layer. The output of each unit in the OL can be calculated through the output of the middle layer and the connection weights, as shown in formula (7).

$$L_t = \sum_{j=1}^p v_{jt} b_j - \gamma_t, t = 1, 2, \dots, q \quad (7)$$

In formula (7), L_t represents the output of each unit in the OL. v_{jt} represents the connection weight. γ_t represents the threshold. The output calculation of each unit in the OL is used to calculate the response of each unit in the OL, as shown in formula (8).

$$C_t = f(L_t), t = 1, 2, \dots, q \quad (8)$$

In formula (8), C_t represents the response of each unit in the OL. Based on the real output and the objective vector, the generalization error of each unit in the OL can be calculated, as shown in formula (9).

$$d_t^k = (y_t^k - C_t) \cdot C_t \cdot (1 - C_t), t = 1, 2, \dots, q \quad (9)$$

In formula (9), d_t^k represents the generalized error of

each unit in the OL. y_i^k represents the objective vector.

Based on the connection weights, the generalization error of the OL, the output of the middle layer, and the generalization error in the middle layer can be calculated, as displayed in formula (10).

$$e_j^k = \left[\sum_{i=1}^q d_i^k \cdot v_{ji} \right] b_j (1 - b_j) \quad (10)$$

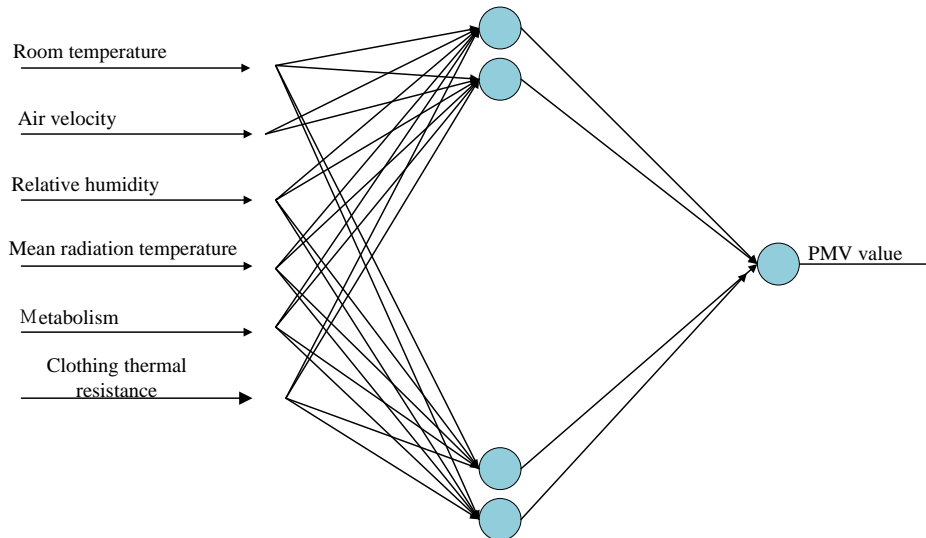


Figure 3: BPNN structure for predicting PMV

Figure 3 displays the BPNN structure for predicting PMV indicators. The input of the model is the six factors of operating thermal comfort index. The output is the PMV indicators. The network structure contains a neuron, with a BPNN input layer of 6 dimensions and an OL of 1 dimension.

In formula (10), e_j^k represents the generalized error in the middle layer. Formulas (5)-(10) are forward propagation process, followed by back propagation process. By adjusting the generalization error and each unit's output in the OL, as well as the generalization error and each unit's output in the middle layer, the connection weights and thresholds are corrected. Relying on the thermal comfort index, the prediction model is shown in Figure 3.

3.2 Optimization of BPNN model combined with GA

There are defects in BPNN, such as long training time, large errors, and susceptibility to local minima. Therefore, GA is used to optimize it. GA is widely used in model optimization, because GA has better global search ability in discontinuous spaces [19-20]. GA follows the survival of the fittest. Genetic operators perform selection, crossover, and mutation to create a new group of solutions, ultimately completing optimization. The process of GA is shown in Figure 4.

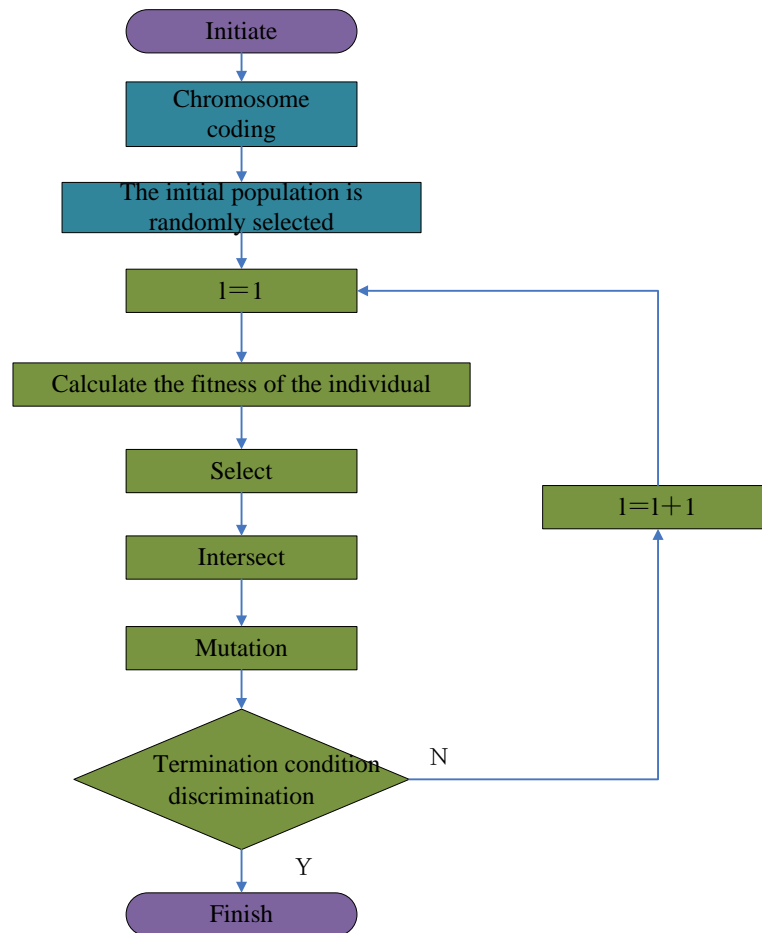


Figure 4: GA basic flow chart

Figure 4 shows the basic process of GA. The initial population of GA is generated through encoding, which is a prerequisite for GA solving and affects the cross mutation. GA first initializes the population, randomly generates string structured data, and uses it as the initial point for iteration. At the same time, the maximum evolutionary iteration is set and a random method is applied to generate the initial population. Then, the individual fitness function is calculated, which affects the optimization process and convergence speed. Afterwards, individuals with higher fitness are selected to generate the

new generation of new populations. According to a probability of 0.5-1.0, two individuals are selected to cross, that is, to exchange the corresponding gene combinations on the individuals. After crossing, some individual positions are changed with a small probability. Finally, when the fitness stabilizes and achieves the global optimum, or after achieving the specified number of iterations, the operation stops. Based on the input data from BPNN, the GA-BPNN prediction model for PMV indicators is established, as displayed in Figure 5.

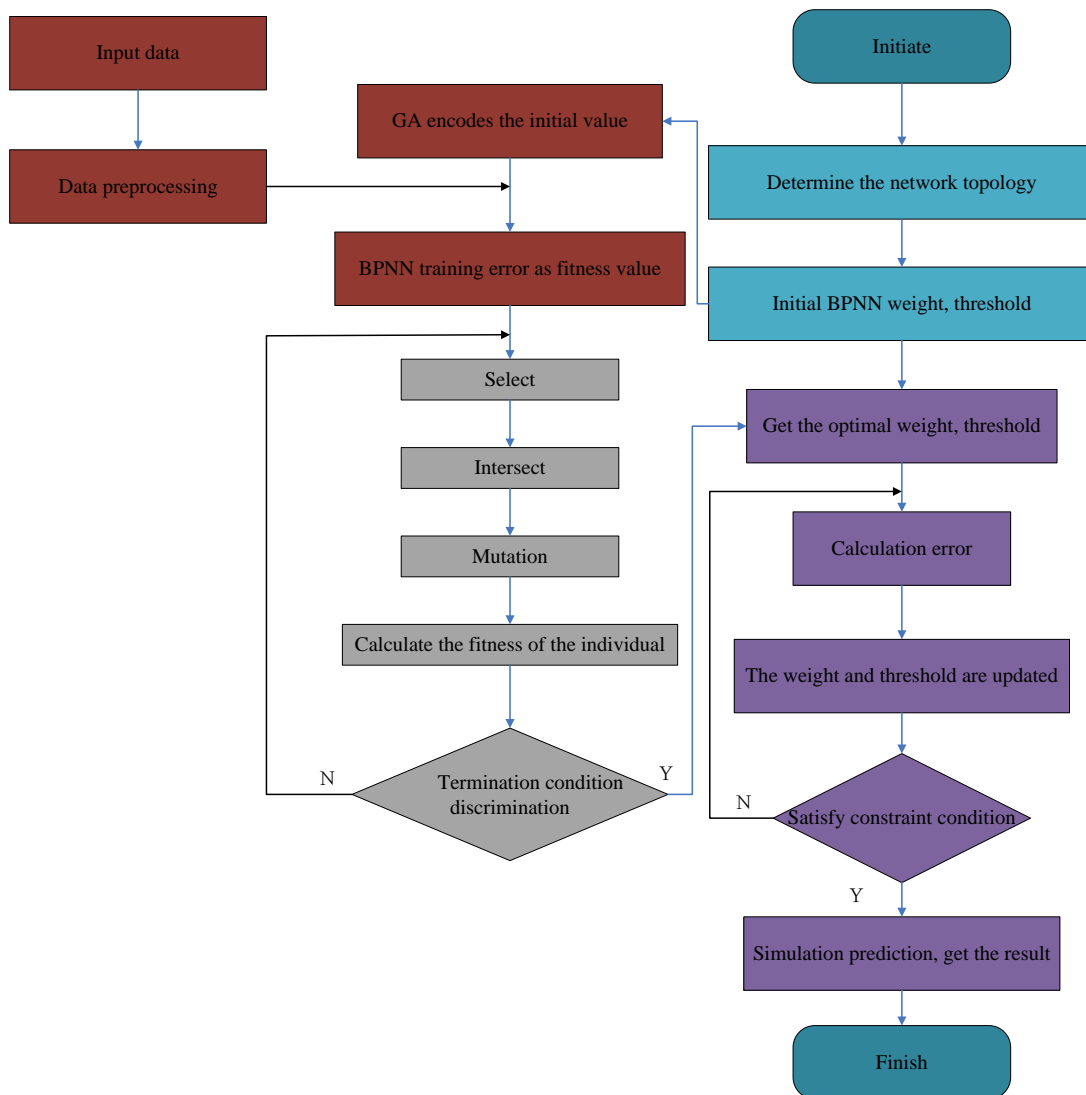


Figure 5: GA-BPNN flowchart

Figure 5 is a schematic diagram of optimized BPNN model based on GA. The entire process starts from the input data and ensures that the data format is suitable for model training through data preprocessing, such as normalization. Next, the network topology of BPNN is determined, including the number of layers and the number of neurons in each layer. The added GA encodes the initial weights and thresholds of BPNN to form the initial population. These encoded individuals evaluate fitness by calculating BPNN training errors, with smaller errors indicating higher fitness. Based on the fitness, GA performs selection operations to select the best individuals for crossover and mutation, in order to generate new offspring populations, enhance the model's generalization ability, and avoid falling into local optima. During the iteration process, newly generated individuals are evaluated based on their fitness, and the weights and thresholds of BPNN are updated accordingly. This process is repeated until the preset termination conditions are met, such as reaching the maximum number of

iterations or fitness reaching the predetermined threshold. In addition, the process also includes checking the constraints of the solution to ensure that the found solution not only has high fitness but also satisfies all the constraints of the problem. Finally, the optimized BPNN model is used for simulation prediction, resulting in more accurate prediction results. The relationship between the length of the encoding string and BPNN is expressed as formula (11).

$$S = m \times h + h \times n + h + n \quad (11)$$

In formula (11), $m \times h$ represents the encoding length of the connection weight in the input layer and HL. $h \times n$ represents the encoding length of the weight between the HL and the OL. h represents the encoding length of the HL threshold. n represents the encoding length of the OL threshold. According to the BPNN model, the input layer has 6 parameters, and the HL is 10. The OL has a PMV value. Therefore, the encoding length is calculated, and $S = 6 \times 10 + 10 \times 1 + 10 + 1 = 81$. The initial population consists of N randomly generated numerical particles.

The population size refers to the number of individuals included. Fitness measures the individual superiority or inferiority in GA. Individual fitness values have an impact on the probability they leave behind. Individuals with higher fitness are closer to the optimal solution. BPNN is actually the process of finding the optimal solution. Nonlinear transformation generates output values. The actual and output value errors are transmitted in reverse. The weights and thresholds are modified to ultimately output the weights and thresholds that achieve the minimum error. The mean square error of BPNN is displayed in formula (12).

$$E = \frac{1}{2m} \sum_{k=1}^m \sum_{o=1}^q [d_o(k) - y_o(k)]^2 \quad (12)$$

Based on the above analysis, the reciprocal mean square error of BPNN can serve as the fitness function of GA. It can distinguish individual strengths and weaknesses. The fitness function of GA is expressed as formula (13).

$$fitness = \frac{1}{E} = \frac{1}{\frac{1}{2m} \sum_{k=1}^m \sum_{o=1}^q [d_o(k) - y_o(k)]^2} \quad (13)$$

In formula (13), *fitness* represents the fitness function. A higher fitness function value indicates good individual fitness and superior algorithm performance, while the opposite indicates poorer performance. The main step of crossover in GA is to randomly pair particles with high fitness in the population. Genes are crossed to form new individuals. Crossover operation is shown in formula (14).

$$\begin{aligned} a_{kj} &= a_{kj}(1-b) + a_j b \\ a_{ij} &= a_{ij}(1-b) + a_k b \end{aligned} \quad (14)$$

In formula (14), a_k and a_i represent different chromosomes that undergo crossover operations at position j . b represents a random number between 0 and 10. Mutation operation is carried out after crossover to alter individual genes and prevent the optimization

process from converging in the immature stage. The mutation form is shown in formula (15).

$$a_{ij} = \begin{cases} a_{ij} + (a_{ij} - a_{\max}) \times f(g) & r > 0.5 \\ a_{ij} + (a_{\min} - a_{ij}) \times f(g) & r \leq 0.5 \end{cases} \quad (15)$$

In formula (15), a_{ij} represents the j -th gene of the i -th individual. a_{\min} represents the minimum lower bound of a_{ij} . a_{\max} represents the maximum upper bound value of a_{ij} . $f(g) = r_2(1 - g/G_{\max})$. r_2 represents a randomly generated number. G_{\max} represents the maximum iteration times. g represents the population iteration. r refers to a random number between 0 and 1.

4 Analysis of GA-BPNN model based on perception and behavior correlation

The study analyzes the proposed model in two parts. Firstly, the BPNN model is compared to verify its effectiveness. Then it is compared with other models to verify its superiority.

4.1 Optimization Analysis of GA-BPNN Model

To test the proposed model, the topology parameters of the BPNN remain unchanged. The maximum iteration time for GA is 200, and the population size is 50. The fitness function takes the derivative of the prediction error of the BPNN, with a crossover probability of 0.4 and a mutation probability of 0.2. The study selects a thermal comfort index database from a certain university, with a data sample of 2000 groups, which is separated into training and testing samples according to a 9:1 ratio. Firstly, all data is standardized and normalized. The laboratory environment settings are shown in Table 2.

Table 2: Laboratory environment setting

Hardware and software configuration	Version model
CPU	Intel(R)Core i7-7700@3.6GHz
Operating system	Ubuntu 18.04 LTS
CUDA	9.1
Deep learning frameworks	Pytorch1.10
Python version	3.7

Table 2 displays the experimental settings in the laboratory. Experiments are conducted on BPNN and GA-BPNN. The fitness curve is shown in Figure 6.

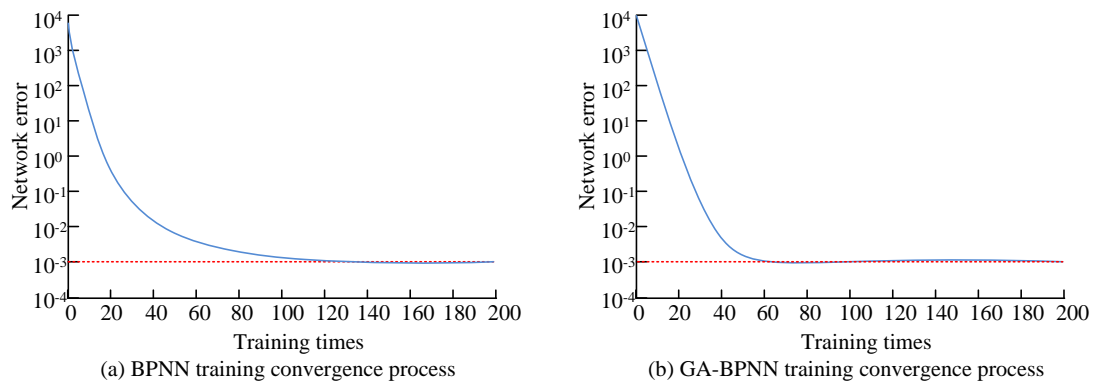
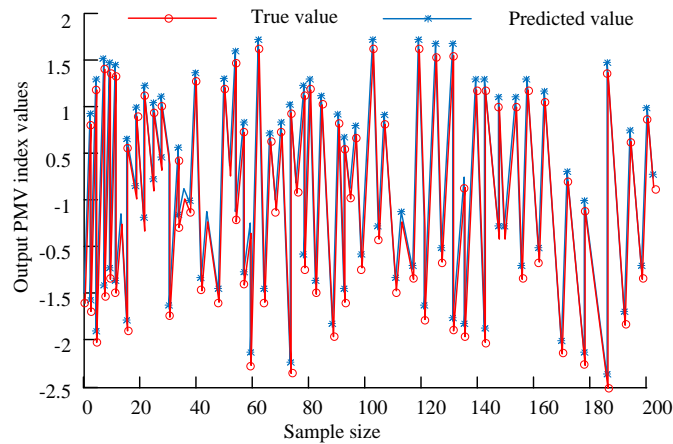


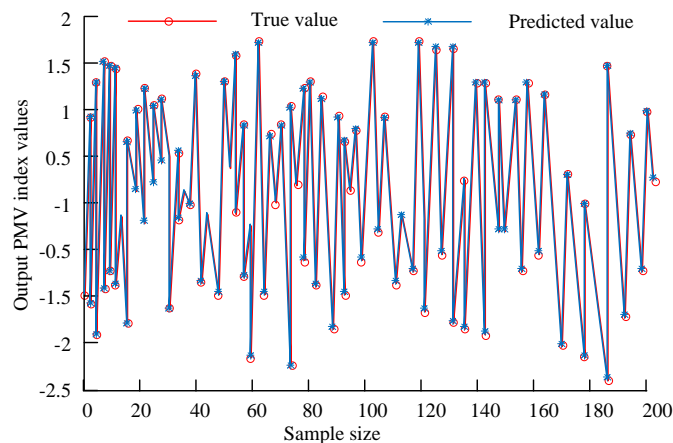
Figure 6: GA-BPNN and BPNN training convergence process diagram

Figure 6 (a) presents the convergence process of BPNN training. Figure 6 (b) presents the convergence process of GA-BPNN training. From the Figure, BPNN and GA-BPNN gradually converged with increasing training times. For the BPNN, it quickly converged in the first 60 training times, then converged around 100 training times,

and the network error stabilized at 10^{-3} . For the GA-BPNN, the convergence speed was fast in the first 40 training times, converged around 60 training times, and the network error stabilized at 10^{-3} . The BPNN model improved by GA has a fast convergence speed. Two models are further experimented, as shown in Figure 7.



(a) BPNN comparison of true value and predicted value



(b) GA-BPNN comparison of true value and predicted value

Figure 7: Comparison of actual and predicted values between GA-BPNN and BPNN

Figure 7 (a) displays the actual and predicted values of BPNN, which had a significant deviation, with poor fitting effect. Figure 7 (b) displays the comparison results

of GA-BPNN. The difference of PMV was small, and the model fitting effect was better. The error curves of the two models are shown in Figure 8.

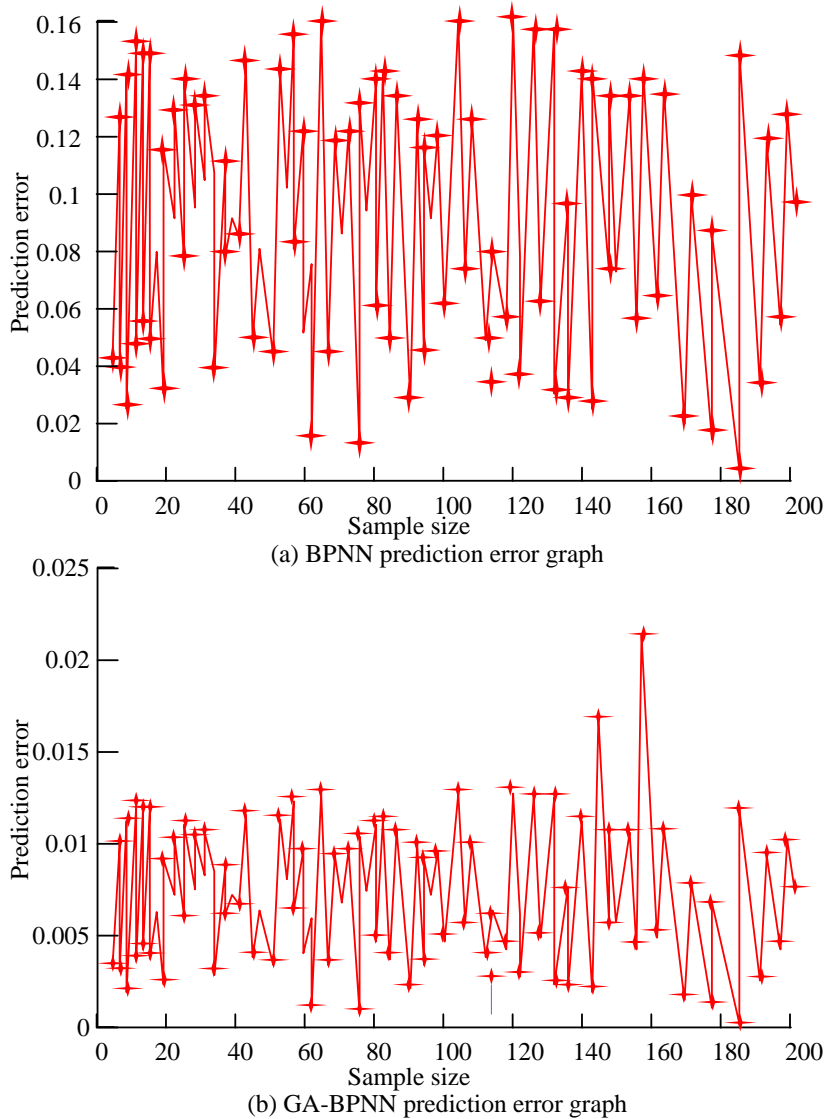


Figure 8: GA-BPNN and BPNN error curves

Figure 8 (a) shows the BPNN error curve. From the Figure, the BPNN model had a large error in PMV prediction, with the error basically remaining around 0.1 and the maximum error reaching 0.16. Figure 8 (b) shows the GA-BPNN error curve. Compared with the BPNN model, the GA-BPNN model generally maintained lower error, with an error of around 0.01 and a maximum error of only 0.022. The PMV had a large number of input samples. The BPNN model made the training objectives more complex, with longer runtime and lower efficiency. There is over fitting during the training process, resulting in poor model prediction performance. GA improves the BPNN model by optimizing weights and thresholds,

reducing unnecessary training, and achieving good fitting results, which is an effective improvement.

4.2 Performance analysis of GA-BPNN model

The proposed method is compared with other intelligent environment design methods that can be used to combine PMV indicators in experiments. The selected comparison models include Support Vector Machine (SVM), Convolutional Neural Network (CNN), Recurrent Neural Network (RNN), and GA-Recurrent Neural Network (GA-RNN). The SVM is a supervised learning strategy commonly used for data classification and regression

analysis. SVM classifies data by mapping it to a high-dimensional space and finding a hyperplane that maximizes the interval. The core of the CNN is a network structure that includes three layers. It extracts features from input data through convolutional operations, reduces the feature map dimensionality through pooling operations, and finally performs classification or regression tasks through fully connected layers. The RNN has a recurrent neural network structure, which can handle serialized data and preserve previous information. The GA-RNN combines GA and RNN. The GA is adopted to upgrade the parameters of RNN, which can find the optimal RNN structure and hyper-parameters to optimize the performance. The study selects Accuracy, Precision, F1-score, RMSE, and R-squared as model validation indicators. Accuracy is the most intuitive

performance indicator, which represents the proportion of correctly predicted samples in the model to the total number of samples. Precision measures the proportion of positive classes predicted by the model, that is, how many of the predicted positive categories are accurate. The F1-score is the harmonic mean of precision and recall (accuracy), which strikes a balance between the two. It is a comprehensive indicator that considers both precision and recall. A high F1-score indicates higher precision and recall of the model. RMSE is a commonly used indicator to measure the error between model predictions and observations. R-squared is the determination coefficient that represents the degree to which the model explains the variability of observations. The proposed method is compared with comparison models in the laboratory. Figure 9 displays the results.

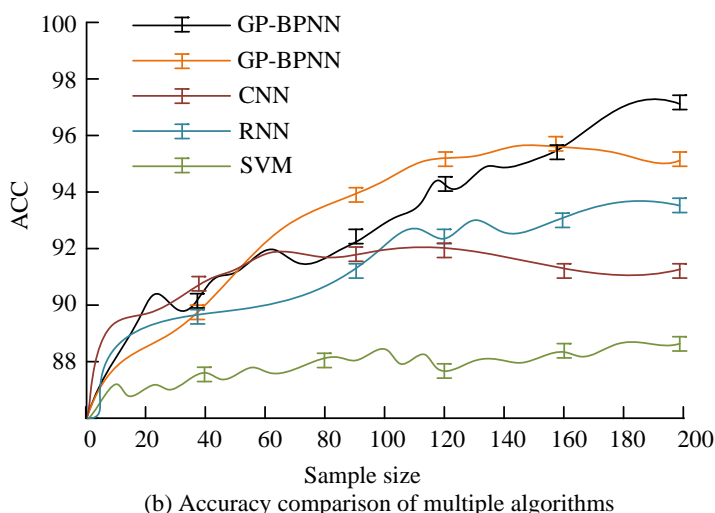
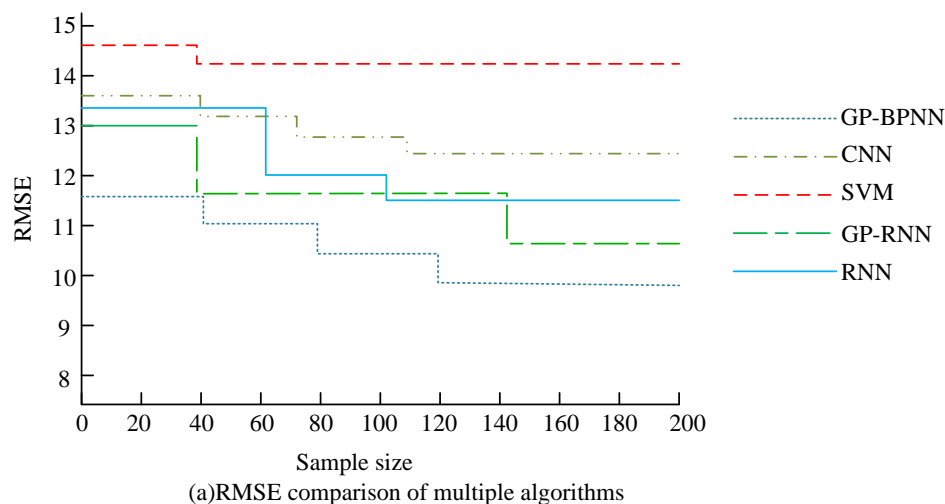


Figure 9: Comparison of RMSE and Accuracy of various models

Figure 9 (a) displays the RMSE results of multiple algorithms. From the Figure, the proposed model had the lowest RMSE, while the SVM had the highest, indicating that the difference was small, and the predictive ability

was good. The SVM model had a significant difference, with poor predictive ability. Figure 9 (b) shows the Accuracy comparison results of multiple algorithms. The proposed model had high Accuracy. In addition, the

GA-RNN model also had high Accuracy. Table 3 presents the results of other indicators.

Table 3: Comparison results of multiple models

Model	Accuracy	Precision	F1-score	RMSE	R-square
SVM	88.23%	89.71%	0.714	14.29	0.73
CNN	91.94%	89.97%	0.753	12.54	0.81
RNN	93.67%	91.02%	0.787	11.60	0.76
GA-RNN	95.62%	92.36%	0.815	10.73	0.93
GA-BPNN	97.89%	96.15%	0.896	10.03	0.92

Table 3 compares other indicators of multiple models. From the data in the table, the proposed model achieved higher Accuracy, Precision, and F1-score, with values of 97.89%, 96.15%, and 0.896. Compared with the GA-BPNN, the GA-RNN presented a decrease in Accuracy, Precision, and F1-score. In terms of RMSE, the GA-RNN and GA-BPNN had lower values of 10.73

and 10.03, respectively. For the R-square, the GA-RNN model reached the highest, at 0.93, while the GA-BPNN decreased slightly but also maintained a high level. This indicates that the GA-BPNN and GA-RNN can effectively explain the changes in observed data, thereby accurately predicting comfort feelings under different environmental conditions. The comparison of network fitness is shown in Figure 10.

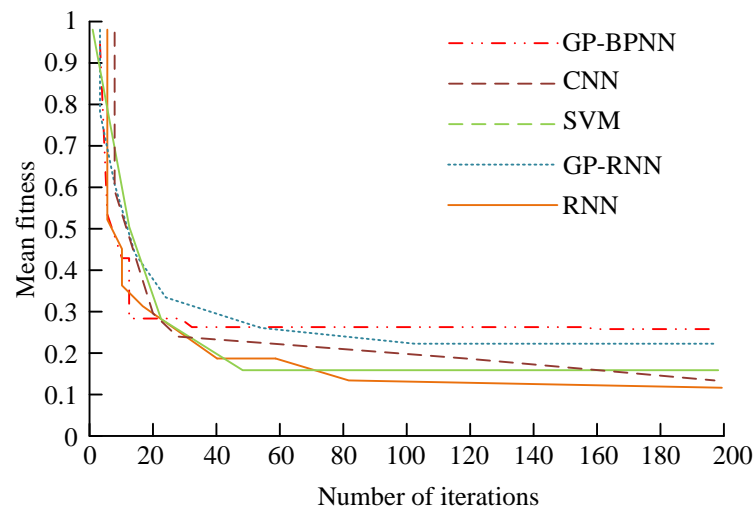


Figure 10: Multiple model network fitness curves

Figure 10 shows the fitness curves. The GA-BPNN model exhibited significant changes in 0-20 iterations, gradually stabilizing at 40 iterations and finally stabilizing at 0.26. The GA-RNN model showed significant changes in 0-60 iterations. Thereafter, its fitness remained stable at 0.24. The fitness of RNN, CNN, and SVM was relatively low, which stabilized at 0.12, 0.13, and 0.17. The GA-BPNN model has good generalization ability and better predictive performance. The performance of RNN, CNN, and SVM is not ideal enough to achieve prediction results.

5 Conclusion

A GA-BPNN prediction model based on perception and behavior correlation was constructed to achieve intelligent environment design in indoor spaces. PMV is a crucial component in indoor intelligent environments.

The factors affecting PMV were analyzed. Then the BPNN model was introduced to predict PMV indicators. However, the BPNN model has drawbacks such as long training time, large errors, and the tendency to fall into local minima. Therefore, the GA was introduced to improve it, and the GA-BPNN model was constructed. The effectiveness of the improvement was verified. Then the superiority of the model through comparative experiments was proved. The experimental results showed that the GA-BPNN converged faster than the BPNN. The difference of PMV was small, with better model fitting effects. The BPNN had a significant error in PMV prediction, with an error of around 0.1 and a maximum error of 0.16. The overall error of the GA-BPNN remained at a relatively low level, with an overall error of around 0.01 and a maximum error of only 0.022. Compared with other models, the GA-BPNN had higher Accuracy, Precision, and F1-score, with values of

97.89%, 96.15%, and 0.896, respectively. The GA-BPNN showed significant changes in fitness during the first 20 iterations, with the fitness value ultimately stabilizing at 0.26, indicating good generalization ability and predictive performance. The proposed model achieves intelligent design of indoor comfort by controlling temperature. However, the factors that affect PMV indicators are not limited to temperature. In subsequent research, the optimal combination of environmental parameters can be adjusted to improve indoor intelligence.

6 Discussion

The GA-BPNN model based on perception and behavior correlation proposed in the study has demonstrated advantages in the intelligent indoor environment design. By comparing with relevant works in existing literature, the contributions and advantages of this study can be more clearly identified. Compared with the car following model proposed by Wang W J et al. in intelligent transportation systems, the designed model focuses on predicting the thermal comfort of indoor environments. Although both adopt simulation and optimization strategies, the research method combines the global search ability of GA and the learning ability of BPNN, particularly targeting the optimization of PMV indicators, which is an innovative application in indoor environment design. Compared with the behavior prediction model proposed by Cheng et al. in intelligent butler design, the proposed model not only predicts user behavior, but also further predicts the impact of these behaviors on indoor environmental comfort. The BPNN optimized by GA shows faster convergence speed and higher accuracy in predicting PMV indicators, which is clearly reflected in the comparison results of Figure 6 and Figure 7. In addition, the designed model outperforms the intelligent reflective/refractive surface assisted high mobility communication system proposed by Huang Z et al. in terms of accuracy, precision, and F1-score. In Table 2, the GA-BPNN model has higher reliability and effectiveness in predicting indoor environmental comfort, with scores of 97.89%, 96.15%, and 0.896 on these indicators, respectively. Compared with the BPNN-based multi-body dissipative particle dynamics calibration method proposed by Yu X et al., the GA-BPNN model exhibits stronger robustness and adaptability in dealing with nonlinear problems and multivariate optimization. Through GA optimization, the model not only avoids getting stuck in local minima, but also improves the accuracy and efficiency of indoor environment control. Overall, the GA-BPNN model proposed in the study provides a new solution for intelligent design of indoor environments. This model not only improves the accuracy of PMV indicator prediction, but also provides strong technical support for achieving automation and intelligence of indoor comfort through intelligent temperature control.

Fundings

The research is supported by Fujian Provincial Education Science "14th Five-Year Plan" 2021 Annual Project: Exploration and Practice of Practice Based Talent Cultivation Mode for Environmental Design Majors in Universities under the Background of Rural Revitalization Strategy (Fund Number: FJJKBK21-167).

References

- [1] X. M. Long, Y. J. Chen, and J. Zhou, "Development of AR experiment on electric-Thermal effect by open framework with Simulation-Based asset and User-Defined input," *Artificial Intelligence and Applications*, vol. 1, no. 1, pp. 52-57, 2023. <https://doi.org/10.47852/bonviewAIA2202359>
- [2] J. He, K. Yu, Y. Shi, Y. Zhou, W. Chen, and K. B. Letaief, "Reconfigurable intelligent surface assisted massive MIMO with antenna selection," *IEEE Transactions on Wireless Communications*, vol. 21, no. 7, pp. 4769-4783, 2021. <https://doi.org/10.1109/TWC.2021.3133272>
- [3] M. Cucchi, D. Parker, E. Stavrinidou, P. Gkoupidenis, and H. Kleemann, "In Liquido computation with electrochemical transistors and mixed conductors for intelligent bioelectronics," *Advanced Materials*, vol. 35, no. 15, pp. 2209516-2209530, 2023.
- [4] Z. Feng, B. Clerckx, and Y. Zhao, "Waveform and beamforming design for intelligent reflecting surface aided wireless power transfer: Single-user and multi-user solutions," *IEEE Transactions on Wireless Communications*, vol. 21, no. 7, pp. 5346-5361, 2022. <https://doi.org/10.1109/TWC.2021.3139440>
- [5] L. Zhang, X. Yang, H. Liu, H. Zhang, and J. Cheng, "Efficient residual shrinkage CNN denoiser design for intelligent signal processing: Modulation recognition, detection, and decoding," *IEEE Journal on Selected Areas in Communications*, vol. 40, no. 1, pp. 97-111, 2021. <https://doi.org/10.1109/JSAC.2021.3126074>
- [6] X. Lu, W. Liao, Y. Zhang, and Y. Huang, "Intelligent structural design of shear wall residence using physics-enhanced generative adversarial networks," *Earthquake Engineering & Structural Dynamics*, vol. 51, no. 7, pp. 1657-1676, 2022. <https://doi.org/10.1002/eqe.3632>
- [7] W. J. Wang, M. H. Ma, S. D. Liang, G. Y. Ma, and Y. S. Wang, "Density waves in an improved car-following model under intelligent transportation system environment," *Modern Physics Letters B*, vol. 36, no. 15, pp. 2250014-2250032, 2022. <https://doi.org/10.1142/S0217984922500142>
- [8] S. T. Cheng, C. Hsu, G. J. Horng, and K. T. Tsai, "Quadro-W learning for human behavior prediction in an evolving environment: a case study of the intelligent butler technology," *The Journal of Supercomputing*, vol. 79, no. 6, pp. 6309-6346,

2023. <https://doi.org/10.1007/s11227-022-04899-1>
- [9] Z. Huang, B. Zheng, and R. Zhang, “Transforming fading channel from fast to slow: Intelligent refracting surface aided high-mobility communication,” *IEEE Transactions on Wireless Communications*, vol. 21, no. 7, pp. 4989–5003, 2021. <https://doi.org/10.1109/TWC.2021.3135685>
- [10] R. Zhong, X. Liu, Y. Liu, Y. Chen, and X. Wang, “Path design and resource management for NOMA enhanced indoor intelligent robots,” *IEEE Transactions on Wireless Communications*, vol. 10, no. 21, pp. 8007–8021, 2022. <https://doi.org/10.1109/TWC.2022.3163422>
- [11] X. Yu, J. Zhao, S. Chen, D. Huang, K. Zhang, and D. Cao, “The calibration for many-body dissipative particle dynamics by using back-propagation neural networks,” *Molecular Simulation*, vol. 48, no. 11, pp. 955–964, 2022. <https://doi.org/10.1080/08927022.2022.2055755>
- [12] Z. Sui, J. Mu, T. Wang, and S. Zhang, “Evaluation of energy saving of residential buildings in North China using back-propagation neural network and virtual reality modeling,” *Journal of Energy Engineering*, vol. 148, no. 3, pp. 4022013–4022025, 2022. [https://doi.org/10.1061/\(ASCE\)EY.1943-7897.0000832](https://doi.org/10.1061/(ASCE)EY.1943-7897.0000832)
- [13] L. Zhang, K. Jiao, L. Zhang, J. Zhang, M. Sun, and Z. Zhou, and A. Zheng, “Prediction of blast furnace fuel ratio based on back-propagation neural network and K-Nearest neighbor algorithm,” *Steel Research International*, vol. 93, no. 10, pp. 2200215–2200226, 2022. <https://doi.org/10.1002/srin.202200215>
- [14] Y. Xu, Z. Liu, Q. Zhang, F. Guan, Z. Yan, B. Huang, A. Pan, J. Hu, Z. Chen, Q. Ding, X. Qiu, and Y. Tang, “A geomagnetic vector compensation method compatible with nonlinear interferences based on back propagation network and 3D Helmholtz coil,” *Review of Scientific Instruments*, vol. 94, no. 3, pp. 35111–35119, 2023. <https://doi.org/10.1063/5.0138606>
- [15] J. Zolgharnein, T. Shariatmanesh, S. D. Farahani, “Artificial neural network (ANN) modeling for simultaneous removal of a binary mixture of Pb (II) and Cu (II) by cobalt hydroxide nano-flakes,” *Journal of Chemometrics*, vol. 37, no. 4, pp. 3475–3485, 2023. <https://doi.org/10.1002/cem.3475>
- [16] X. Yu, J. Zhao, S. Chen, D. Huang, K. Zhang, and D. Cao, “The calibration for many-body dissipative particle dynamics by using back-propagation neural networks,” *Molecular Simulation*, vol. 48, no. 11, pp. 955–964, 2022. <https://doi.org/10.1080/08927022.2022.2055755>
- [17] G. Veselov, A. Tselykh, A. Sharma, and R. Huang, “Applications of artificial intelligence in evolution of smart cities and societies,” *Informatica*, 45(5), pp. 603, 2021. <https://doi.org/10.31449/inf.v45i5.3600>
- [18] F. Zeng, R. Wan, Y. Xiao, F. Song, C. Peng, and H. Liu, “Predicting the Self-Diffusion coefficient of liquids based on backpropagation artificial neural network: A quantitative Structure–Property relationship study,” *Industrial & Engineering Chemistry Research*, vol. 61, no. 48, pp. 17697–17706, 2022. <https://doi.org/10.1021/acs.iecr.2c03342>
- [19] J. Ding, R. Alroobaea, A. M. Baqasah, A. Althobaiti, and R. Miglani, “Big data intelligent collection and network failure analysis based on artificial intelligence,” *Informatica*, vol. 46, no. 3, pp. 253–392, 2022. <https://doi.org/10.31449/inf.v46i3.3866>
- [20] L. Yang, K. Wang, and H. Sun, “A grating lobe suppression method for displaced subarrays using genetic algorithm,” *IET Microwaves, Antennas & Propagation*, vol. 16, no. 7, pp. 457–464, 2022. <https://doi.org/10.1049/mia2.12258>